Available online at www.sciencedirect.com
SCIENCE DIRECT®
Journal of Human Evolution 46 (2004) 655–677

Effects of food processing on masticatory strain and craniofacial growth in a retrognathic face

Daniel E. Lieberman[a]*, Gail E. Krovitz[b], Franklin W. Yates[a], Maureen Devlin[a], Marisa St. Claire[c]

[a] *Department of Anthropology, Peabody Museum, Harvard University, 11 Divinity Avenue, Cambridge, MA 02138, USA*
[b] *Department of Anthropology, 409 Carpenter Building, Penn State University, College Park, PA 16802, USA*
[c] *Bioqual Corporation, 9600 Medical Center Drive, Rockville, MD 20850-3336, USA*

Received 17 November 2003; accepted 19 March 2004

Abstract

Changes in the technology of food preparation over the last few thousand years (especially cooking, softening, and grinding) are hypothesized to have contributed to smaller facial size in humans because of less growth in response to strains generated by chewing softer, more processed food. While there is considerable comparative evidence to support this idea, most experimental tests of this hypothesis have been on non-human primates or other very prognathic mammals (rodents, swine) raised on hard versus very soft (nearly liquid) diets. Here, we examine facial growth and in vivo strains generated in response to raw/dried foods versus cooked foods in a retrognathic mammal, the rock hyrax (*Procavia capensis*). The results indicate that the hyrax cranium resembles the non-human primate cranium in having a steep gradient of strains from the occlusal to orbital regions, but differs from most non-anthropoids in being primarily twisted; the hyrax mandible is bent both vertically and laterally. In general, higher strains, as much as two-fold at some sites, are generated by masticating raw versus cooked food. Hyraxes raised on cooked food had significantly less growth (approximately 10%) in the ventral (inferior) and posterior portions of the face, where strains are highest, resembling many of the differences evident between humans raised on highly processed versus less processed diets. The results support the hypothesis that food processing techniques have led to decreased facial growth in the mandibular and maxillary arches in recent human populations.

Keywords: Hyrax; Skull growth; Mandible; Maxilla; Cooking; Mastication; Strain

Introduction

Understanding how the face resists and responds to masticatory forces is important for testing hypotheses about the effects of chewing on facial growth. While multiple genetic and

* Corresponding author. Tel.: +1-617-495-5470; fax: +1-617-496-8041
E-mail address: danlieb@fas.harvard.edu (D.E. Lieberman).

0047-2484/04/$ - see front matter © 2004 Elsevier Ltd. All rights reserved.
doi:10.1016/j.jhevol.2004.03.005

environmental factors influence facial growth, several lines of evidence suggest that changes in diet and food processing technology contribute to some proportion of variations in facial size and shape. Human diets since the Middle Paleolithic have changed substantially in content (Stiner et al., 1999; Wrangham et al., 1999; Richards et al., 2001; Stiner, 2001), and in how they are processed through cooking, soaking, leaching, and grinding (Rangel et al., 1985; Brace et al., 1987, 1991; Shiau et al., 1999; Wrangham and Conklin-Brittain, 2003). Food processing improves digestibility, but also makes food softer and smaller in particle size, requiring less occlusal force per chew and fewer chewing cycles per unit of food (Lucas and Luke, 1984; Lukacs, 1989; Lieberman, 1993; Agrawal et al., 1997; Strait, 1997). In turn, softer and more processed foods are widely hypothesized to lead to less facial growth, especially in the lower face and the alveolar crests, because of the potential effects of force-generated strain (see Carlson, 1976; Carlson and Van Gerven, 1977; Corruccini and Beecher, 1982). Strain can stimulate periosteal growth and/or inhibit resorption in skeletally immature animals, perhaps to adapt bone shape and structure so that applied forces elicit strain energies below threshold ranges (Rubin and Lanyon, 1984; Biewener et al., 1986; Martin et al., 1998; Carter and Beaupré, 2001; Currey, 2002; Lieberman et al., 2003). In addition, low magnitudes and frequencies of loading can lead to local bone resorption. Loss of dental function in the mandible can decrease alveolar crest height and ramus length by up to 50% (Carlsson and Persson, 1967; Israel, 1973; Sugimura et al., 1984).

While one might expect nutritional improvements since the Middle Paleolithic to contribute to increases in overall cranial size (see Kiliaridis et al., 1992), the evidence points to a trend towards smaller facial size, with the most dramatic decreases occurring after the Neolithic. Comparisons of Nubian populations prior to and after the introduction of agriculture show significant reductions in many mid- and lower facial dimensions including infraorbital height (7.8%), masseter origin length (26.3%), mandibular corpus length (22%), and mandibular symphysis thickness (15.3%)—despite concurrent increases in brain size (Carlson, 1976; Carlson and Van Gerven, 1977). Similar decreases in mandibular and maxillary arch size, especially in the alveolar crests, occurred over the last century among Australian aborigines and other populations who have transitioned to modern, processed diets (Corruccini, 1984, 1990; Lukacs, 1989). Significant, but less extreme, decreases in facial size are typical in populations following the industrial revolution. For example, a comparison of late medieval and recent Finns (with presumably no major genotypic differences) reveals a 6% decrease in mandible length despite overall skull size increases (Varrela, 1992).

While softer, more processed foods may contribute to facial diminution, few studies have experimentally tested these effects in mammals, only one (Bouvier and Hylander, 1996) quantified growth in response to in vivo strains, and only a few studies have specifically looked at humans. Most human studies have shown that young adults with larger muscle cross-sectional areas and/or higher bite forces have larger, less variably-sized faces than those who produce less bite force (e.g., Ingervall and Helkimo, 1978; Dechow and Carlson, 1983; Kiliaridis et al., 1989; Kiliaridis, 1995; English et al., 2002). Such correlations are difficult to interpret, however, because smaller jaws may result from smaller muscles, but both variables may covary as a result of other factors. Only one study (Ingervall and Bitsanis, 1987) directly quantified human facial growth responses to loading by examining the effects of chewing a hard resinous gum for two hours/day for one year in 13 Greek children between ages 7 and 12. Treatment group individuals were able to produce significantly more force than controls, and had significantly longer mandibular and maxillary arches. No human studies have examined the effects of masticatory loading during early facial growth, when such effects are likely to be greatest, and none have quantified strains or site-specific growth rates.

Most experimental data on facial growth responses to masticatory loading come from studies on non-human anthropoids and other mammalian models. One primate study (Corruccini and Beecher, 1982; Beecher et al., 1983) compared 19 adult squirrel monkeys (*Saimiri sciureus*) raised on

soft food diets with 24 controls raised on hard food diets; another study (Corruccini and Beecher, 1984) compared 16 adult baboons (*Papio cynocephalus*) who were raised on a hard diet for two years with 24 baboons raised on a soft diet. In both studies, animals who chewed harder food had significantly wider and taller faces, thicker mandibular corpora, and taller palates. However, primates raised on softer food often had serious malocclusions from narrowed maxillary arches, rotated and displaced teeth, crowded premolars, and palatal arching, suggesting abnormal growth patterns. A related study on macaques obtained similar results, but also showed that Haversian remodeling rates were higher in monkeys fed hard food (Bouvier and Hylander, 1981, 1996).

Experiments on non-primates reveal a similar picture. Rats raised on soft food have smaller jaw adductor muscles, generate lower mandibular strains, and have significantly decreased anterior facial height, shorter mandibles, and smaller muscle attachment areas (Kiliaridis et al., 1986; Engström et al., 1986; Yamada and Kimmel, 1991). Several studies (Moore, 1965; Kiliaridis, 1989; Kiliaridis et al., 1992) examined interactions between nutrition and strain by comparing mandibular growth in rats whose diets varied in hardness and calcium content. Rats fed low calcium diets had significantly smaller mandibles in all dimensions, whereas the rats fed soft food (regardless of calcium content) had mandibles that were only shorter in vertical height and condyle size. Thus strain and nutrition both influence jaw size, but only strain affects jaw shape. Few controlled studies have been done on larger species. One exception is Ciochon et al. (1997), who compared eight minipigs raised for eight months on nutritionally identical soft and hard diets; the four pigs raised on soft food had serious malocclusions, and differed significantly in facial shape with shorter mandibular rami and narrower midfaces than pigs raised on hard food.

Problems addressed in this study

Two major problems need to be addressed regarding the effects of softer, more processed diets on facial growth in humans. First, most experiments on non-humans have been long-term studies that compared facial growth in subjects fed hard versus extremely soft food, typically chow that was softened to an almost liquid state. As noted above, animals raised on soft food in these studies not only had smaller faces but also developed serious malocclusions from abnormal facial growth. It is not known to what extent these differences resulted from low strains versus a near absence of loading (see Bertram and Swartz, 1991). Obviously, humans raised on cooked food do not typically develop severe facial dysplasia, highlighting the need to examine variations in facial growth in response to treatments that better reflect the effects of food processing technology.

A second problem is that additional experimental data are needed on the relationship between the site specific strain and growth in differently-shaped faces. Many studies, primarily on anthropoids, show that the non-human face is characterized by a steep strain gradient, with high strains near the occlusal plane, moderate strains in the middle face, and low strains in the upper face (Hylander et al., 1991a; Hylander and Johnson, 1992; Ross and Hylander, 1996; Ross, 2001). During unilateral mastication, the zygomatic arch and postorbital septum are subject to bending (Hylander, 1986; Hylander et al., 1991a; Herring et al., 1996; Ross, 2001), and the mandible is subject to a combination lateral transverse bending (wishboning), sagittal bending, and twisting about the longitudinal axis (Hylander, 1979, 1985, 1988; Daegling and Hylander, 1998). There is no consistent evidence for a predominant pattern of deformation in the middle and upper face of primates, in spite of models that the primate face is bent or sheared in the sagittal plane during incision or mastication (see Ross, 2001). Evidence for twisting is mixed. Strains measured in the dorsal interorbital region and the lateral surface of the postorbital in galagos (Ravosa et al., 2000a,b) and the medial orbital wall in owl monkeys and galagos (Ross, 2001) indicate twisting, but circumorbital strains in several non-human anthropoids (*Aotus*, *Macaca*, *Papio*) do not, despite predictions that anthropoids should experience more twisting than strepsirrhines because of more recruitment of balancing side

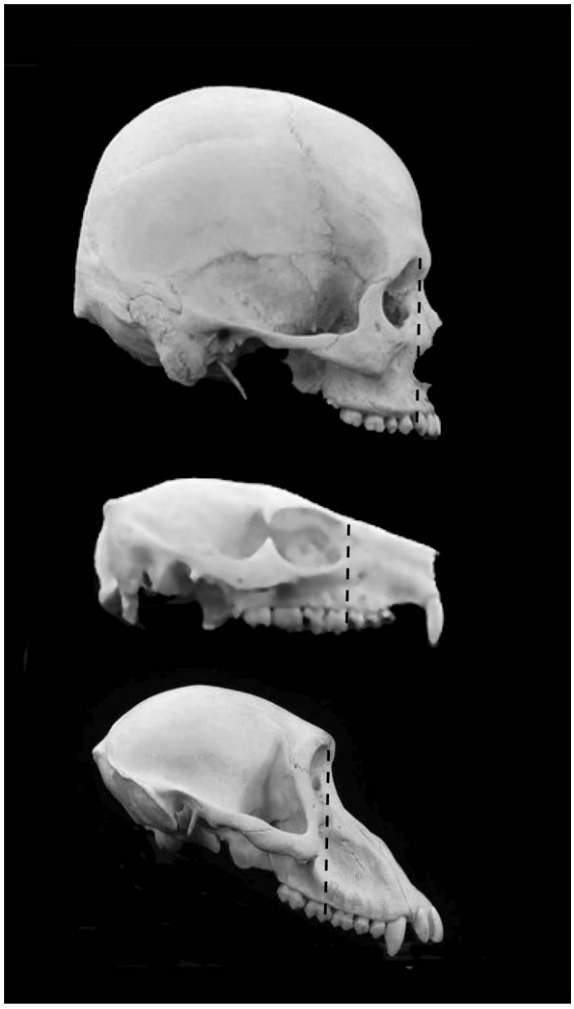

Fig. 1. Lateral views of human (top), rock hyrax (middle), and baboon (bottom) adult skulls scaled to same length. Note that the entire molar row lies beneath or posterior to the plane of the orbits (dashed line) in humans and hyraxes, but not in baboons (which are a particularly prognathic primate). See text for further discussion of craniofacial differences.

adductor force (Hylander et al., 1991a; Ross and Hylander, 1996).

These results raise the question of how variations in facial shape, including the unique architecture of the human face, influence patterns of strain and growth. Compared to other primates, the human face (see Fig. 1) is not only tall, wide, flat and oriented primarily in the coronal plane, but it is also both *retrognathic* (defined here as having postcanine teeth beneath the orbits rather than under a rostrum), and *retracted* (defined here as having the orbits beneath the anterior cranial fossa) (Lieberman and Crompton, 2000). Note that retrognathy as defined here, does not describe the position of the lower face as a whole relative to the upper face (prognathy). Here, we focus on the issue of retrognathy, which is also present in a few non-human anthropoids (e.g., *Saimiri*, *Aotus*). Retrognathy is interesting, in part because the role of the rostrum in dissipating forces generated by mastication or incision in anthropoids is poorly known, and partly because previous studies of in vivo strain in primate faces have not included strain gauges on the rostrum. A number of studies (e.g., Demes, 1982; Greaves, 1985; Preuschoft et al., 1986) have modeled the rostrum as a combination tube and beam that resists twisting around an anteroposterior axis and bending or shearing in the sagittal plane. In addition, Rafferty et al. (2003) have shown that the rostrum in swine is normally subject to shearing forces, but also to torsion during unilateral mastication. It is therefore possible that postcanine retrognathy, in which the occlusion does not occur below a rostrum, may result in a less steep strain gradient because of proportionately more stress transmission from the point of occlusion into the middle and upper portions of the face. In other words, a rostrum may function to dissipate occlusal forces away from the orbital region of the face. If so, then one might also expect unilateral mastication in a retrognathic animal to cause more twisting in the infraorbital, orbital and supraorbital regions.

Theoretically, retrognathy could also affect the absolute forces generated and the relative amount of twisting caused by differential recruitment of balancing versus working side jaw adductors. Depending on muscle position, retracting the postcanine tooth row relative to the TMJ can augment the mechanical advantage of the adductor muscles by reducing load arm length relative to lever arm length. If the adductor muscles generate similar contractile forces (see, however, Demes and Creel, 1988) then mastication could generate higher occlusal forces, hence higher strains in mammals with retrognathic postcanine teeth. Retracting the bite point relative to the TMJ, however, may

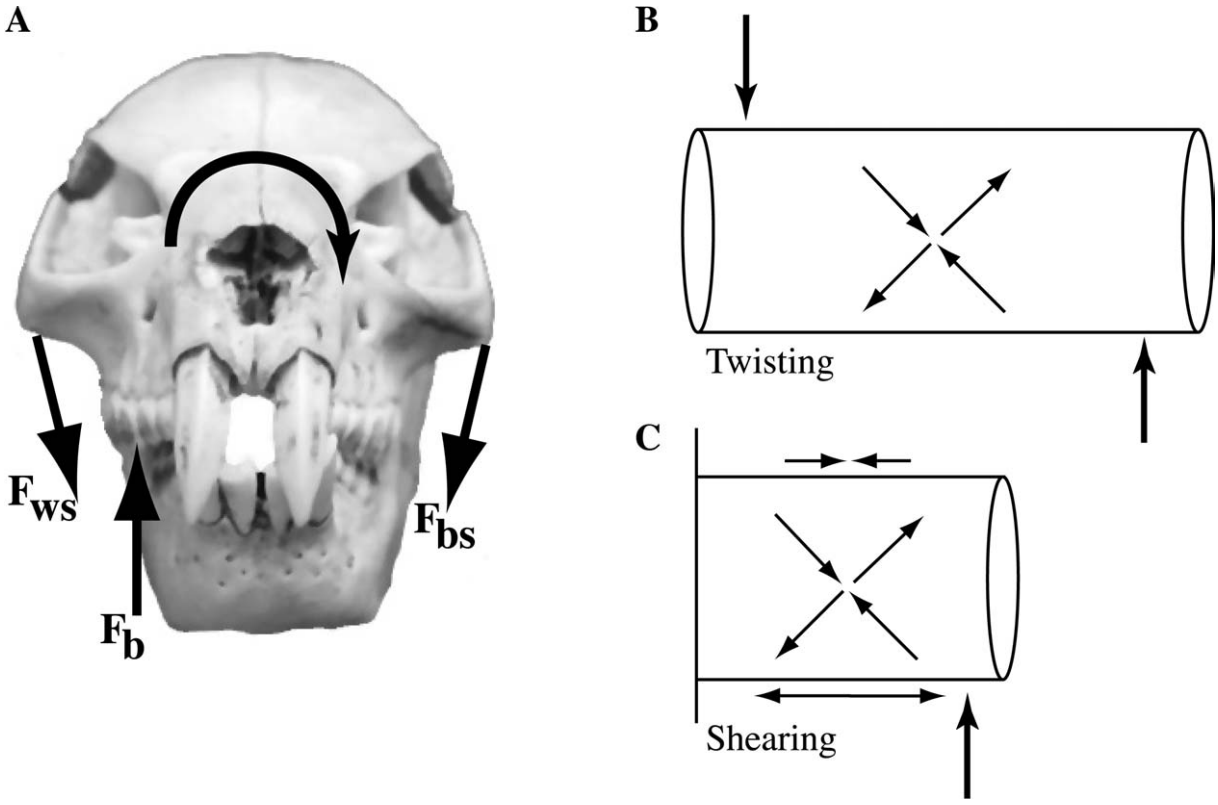

Fig. 2. A, anterior view of hyrax skull showing: F_{ws}, working side masseter force; F_{bs}, balancing side masseter force; F_b, bite force; condylar reaction forces are not shown. B, model of strain orientations during twisting in rostrum; C, model of strain orientations during shearing in rostrum. Divergent arrows indicate tension; convergent arrows indicate compression.

permit less force to be generated, and also has the potential to move the midline resultant of muscle force outside the triangle of support defined by the two TMJs and the bite point (Greaves, 1978), often leading to a reduction in balancing side muscle force when chewing on posterior teeth (Spencer, 1998, 1999). Such reductions might result in less torsion, depending on their relative position along the anteroposterior axis of the face, since working side adductor and occlusal forces tend to cancel each other out (see Fig. 2).

In order to examine effects of cooking and retrognathic faces on facial strain and growth, we present here preliminary data from a non-primate model, the rock hyrax (*Procavia capensis*), which we compare to published data from non-human primates. The hyrax is one of several mammals with substantially retrognathic postcanine dentitions including a few primate species (notably callitrichids and owl monkeys), Proboscidia, some Rodentia (e.g., beavers), and several breeds of dogs (most notably bulldogs and King Charles spaniels). Of these, the hyrax—an herbivorous, sub-ungulate order that includes three genera, *Procavia*, *Dendrohyrax*, and *Heterohyrax*—is a useful experimental model for several reasons. Hyraxes have a generalized, masticatory system (Janis, 1983; Franks et al., 1985), with several morphological similarities to non-human anthropoids. Hyraxes have thin-enameled lophodont molars and premolars, the latter of which are molarized with buccal and lingual wear facets (Janis, 1983). The hyrax mandible has a fused symphysis, a relatively deep and wide mandibular corpus, and an enlarged ascending ramus that provides ample insertion area for a large

masseter-medial pterygoid complex (Janis, 1983). Proportions of the jaw adductor muscles in primates and hyraxes are similar: the masseter and medial pterygoid are the dominant jaw adductors, the temporalis is relatively small, and the has strong divisions between a dorsoventrally oriented superficial portion and a highly transversely oriented deep portion (Janis, 1979, 1983). Electromyogram (EMG) and kinematic data on mastication in the rock hyrax indicate that the power stroke is predominantly transverse, with distinct buccal and lingual phases of occlusion (Wen, 1984; German and Franks, 1991). Although hyraxes have a rostrum (Fig. 1), it is short, and bears only some diminutive premolars, as well as caniniform incisors (no canines) that are not used for unilateral mastication, are rarely used for incision, and instead are mostly used for display, grooming and fighting (Janis, 1979, 1983).

We stress that we do not consider hyraxes an analogy or straightforward model for humans in terms of facial biomechanics. Although hyraxes have retrognathic postcanine teeth and a generally primate-like pattern of chewing, their faces are not retracted below the anterior cranial fossa; they have short infraorbital regions; narrow faces with divergent, non-frontated orbits; and a partially complete postorbital bar, often connected by a substantial postorbital ligament. In addition, the metopic suture remains unfused in hyraxes. Rock hyraxes, however, are otherwise useful as experimental models because they mature rapidly, they are docile if raised in captivity, and able to chew a wide range of diets (Griner, 1968; Rübsamen et al., 1982). The tree hyrax (*Dendrohyrax*) might be a better model because it has complete lateral orbital rims, but this species is not available for experimental studies.

Hypotheses to be tested

The general hypothesis tested here is that mastication of tough, hard foods compared to cooked, soft foods generates higher magnitudes of strains that stimulate more bone growth in the face. This general hypothesis is divided into two sets of specific hypotheses about (1) the pattern of strains generated by masticating different food types, and (2) the effect of strain patterns on regional growth.

In terms of strain, we test two specific hypotheses. First, cooked foods are predicted to generate similar patterns but lower magnitudes of strain than uncooked, raw foods. Second, the pattern of strain in the hyrax face is predicted to follow a gradient characteristic of the primate face in which strains are higher near the site of occlusion and dissipate dorsally away from the tooth row (see Hylander and Johnson, 1992). In terms of osteogenic growth in response to strain, we test three specific hypotheses. First, animals raised on harder, uncooked foods are predicted to have more facial growth than animals raised on softer, more processed foods. Second, variations in the amounts of regional growth in the face are predicted to correlate with strain magnitudes in that region. And third, growth is predicted to occur in the planes of deformation, thereby potentially lowering strain magnitudes.

An additional goal of this study is to relate in vivo strain data from the hyrax to existing models of facial biomechanics, summarized in Figs. 2 and 3, for the cranium and mandible, respectively. If the face and rostrum act like a cylinder that is twisted by a combination of dorsally-directed forces on the working side point of occlusion and ventrally-directed force at both zygomatic arches (Fig. 2a), then principal strains will have similar magnitudes on the balancing and working sides at 45° relative to the long axis in the direction of torsion, with 90° shifts from working to balancing side (Fig. 2b) (see Hylander et al., 1991a). In contrast (or in addition), if the face resists forces as a short beam subjected to bending and/or shearing in the sagittal plane (see Ross, 2001), then the ventral and dorsal aspects will be tensed or compressed, respectively, along their long axes (Fig. 2c).

Models for orientations of strain in the mandibular corpus and symphysis have been outlined in Hylander (1984) and Crompton (1995) and are illustrated in Fig. 3. Bending in the parasagittal plane will cause the ventral margin of the mandibular corpus to experience compression along the long axis (hence tension perpendicular to the long axis) on the balancing side; in contrast, bending will cause the ventral margin of the

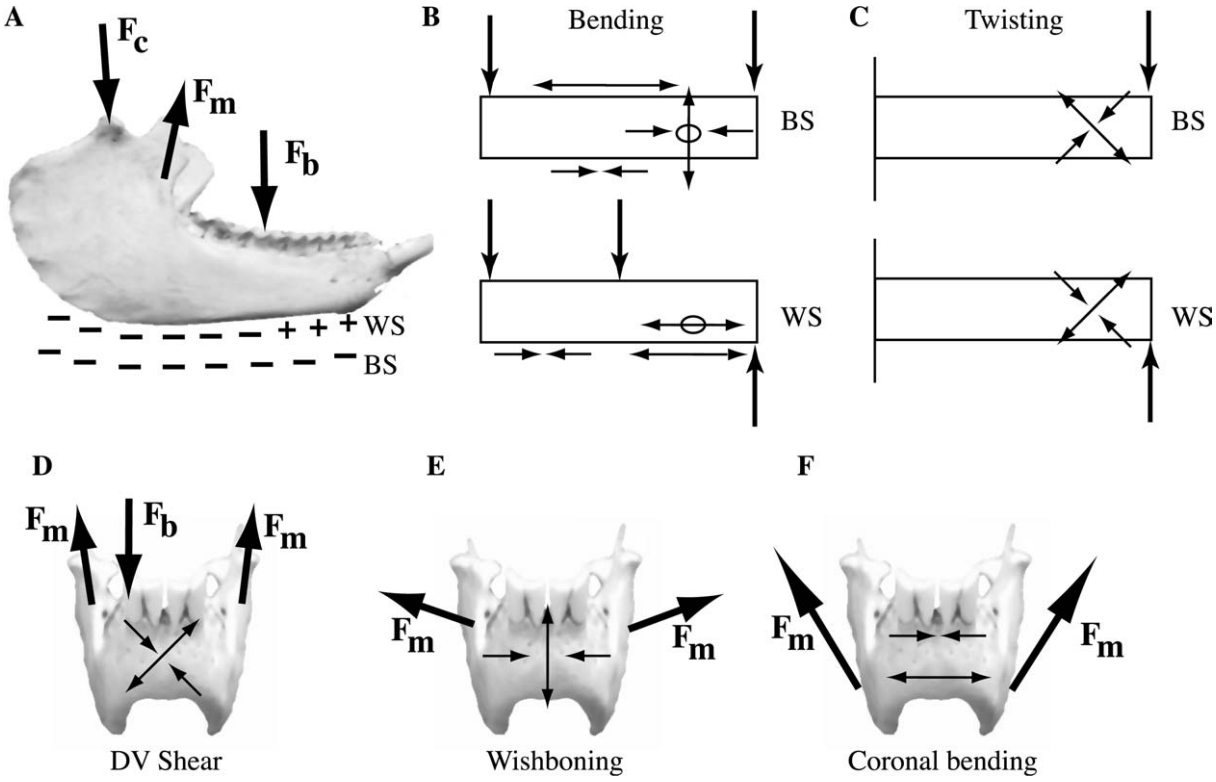

Fig. 3. Simplified biomechanical model of mastication in the hyrax mandible. A, lateral view of hyrax mandible showing: F_c, condylar reaction force (bilateral); F_m, masseter force (bilateral); F_b, bite force. Plus and minus signs denote regions of the ventral margin of the corpus that are compressed or tensed relative to the bite point on the working side (WS) and balancing side (BS). B, Schematic model of strain orientations in the mandibular corpus during bending; C, Schematic model of strain orientations in the mandibular corpus during twisting. D–F, schematic models of strain orientations in the mandibular symphysis during dorso-ventral shear, wishboning (lateral transverse bending), and coronal bending (from twisting of each corpus). Divergent arrows indicate tension, convergent arrows indicate compression. See text for further details.

working side corpus to experience tension along the long axis anterior to the bite point, and compression along the long axis posterior to the bite point (Fig. 3a, b). Twisting of the mandibular corpus around its long axis will cause the orientation of tension to be 45° relative to the long axis in the direction of twisting (Fig. 3c). In the anterior aspect of the symphysis, dorsoventral shear will cause the orientation of tension to be 45° relative to the sagittal plane; lateral transverse bending (wishboning) will mediolaterally compress the symphysis; and twisting of the two corpora will mediolaterally compress the superior margin and mediolaterally tense the inferior margin (what might be called coronal bending) (Fig. 3d–f; for details, see Hylander, 1984).

Materials and methods

Treatment groups

Two groups of rock hyraxes were studied.

Craniofacial growth was examined in a group of eight juvenile hyraxes. These animals were approximately 5–6 months old at the start of the treatment period with unerupted first permanent molars. Treatment period was 98 days. Animals were divided randomly into hard and soft food treatment groups. Both groups were fed the same diet: 1 slice sweet potato (approximately 2″ thick), half of an apple, half a carrot, 1 kale stem (approximately 2″ thick), supplemented with 125 g rabbit chow. In the soft food group, the vegetables were cut into pieces and microwaved for 3–5 minutes

until they were considerably softened, and the rabbit chow was softened through soaking in water. In the hard food group, the vegetables were dehydrated in a Nesco Gardenmaster (Nesco Corp., Twin Rivers, WI) food dessicator for several hours, increasing food toughness and hardness. Both groups were given water ad libitum.

A second group of three adult hyraxes was used solely for strain gauge studies to provide data on magnitude and patterns of strain generated by masticating hard and soft food. These animals were habituated to chew most of the same foods fed to the hard versus soft treatment groups described above (dried and cooked apple, carrot, kale, sweet potato, and lettuce) in a clear plastic box (0.5 m^3). On several occasions, 3 strain gauges were applied surgically to these animals (see below). After recording strains immediately following surgery and on the subsequent day, the strain gauges were removed and the animals allowed to recover for a minimum of six months. Strain gauges were never applied twice to the same location in each animal.

Gauge and electrode application and recording

Small (5 mm^2) rosette (45°) insulated FRA-1-11 rosette strain gauges (Sokki Kenkyujo, Tokyo, Japan) with 120 ± 0.5 Ohm resistance were soldered to 36-gage insulated silver wire (Micro Measurements, Raleigh, NC), sealed with two layers of Micro Measurements A and D coat, and soldered to a 6-pin connector. The orientation of the A-element was painted on the surface of each gauge using metallic ink, and the gauges were sterilized in Betadyne and rinsed in alcohol. In addition, EMG electrodes were made using coated 0.004 mm silver wire (California Fine Wire Co., Laguna Beach, CA) using procedures outlined in Lieberman and Crompton (2000). Animals were fasted for 24 hours prior to surgery; anesthesia was induced with Ketamine (0.2 mg/kg), Xylazine (1.0 mg/kg) and Atropine (0.04 mg/kg), and maintained by Isofluorane (to effect). A maximum of three gauges were applied to each animal at different sites (see below) using a sterile surgical procedure. Each incision site was sterilized, and then perfused with Bupivacaine to provide long-term local anesthesia and minimize swelling. After reflecting any overlying tissue, the periosteum at the gauge site was perfused with Bupivacaine, a small window was cut, and the periosteum removed with a periosteal elevator, and any vessels cauterized. Exposed bone was cleaned with 100% chloroform, and the gauge affixed with methyl-2-cyano-acrylate glue using two minutes of applied pressure. The position of each gauge and the orientation of the A-element was measured relative to standard anatomical planes. The incision was then sutured closed; gauge wires were passed extracutaneously beneath flexible bandages to the back of the neck.

In most animals, EMG electrodes were inserted via a hypodermic needle into the left and right posterior *m. temporalis* to help determine side of chew. Both the EMG and strain gauge connectors were stitched to a surface bandage at the back of the neck (with loops to provide strain relief) and covered with a protective, removable layer of padding.

Six different gauge sites were used (see Fig. 4): (1) the ventral margin of the mandibular corpus below the premolars (thus anterior to most bite points); (2) the ventral margin of the mandibular symphysis; (3) the middle of the zygomatic arch; (4) the dorsal surface of the rostrum lateral and anterior to the premaxillary suture in the plane of the diastema; (5) the interorbital region, just left of the metopic suture; and (6) the interorbital region, on top of the metopic suture.

Following surgery, animals were given a general analgesic (Flunixamine, 1 cc/kg, im), and allowed to recover in a clear plastic feeding box. Strain gauges were connected to a Vishay 2120 Wheatstone bridge amplifier; bridge circuits were balanced and calibrated when the animal was still asleep. EMG wires were connected to a Motion Lab MA 300 EMG amplifier (Motion Analysis, Baton Rouge, LA) with a 60 Hz high-pass filter. Most animals were hungry within a few hours of surgery, and were fed as soon as they were alert. During recording sessions strains and EMG were recorded on a TEAC RD-145T 16 channel digital tape recorder (TEAC Corp, Tokyo, Japan) while the animals were chewing various food items. EMG amplifications were adjusted at the

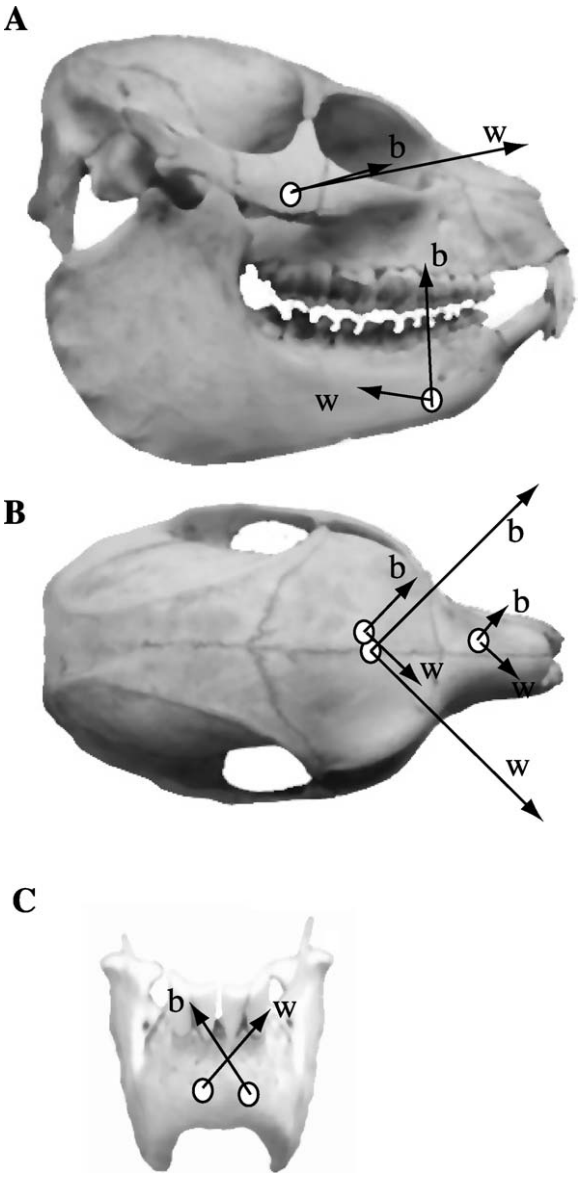

Fig. 4. Locations of strain gauges used in experiment, and mean orientations of principal strain orientation ($\varepsilon_1°$) during mastication of hard food at each location during working (*w*) and balancing (*b*) side chews. Arrow lengths are only approximately proportional to shear (γ) magnitudes. See tables for variation in orientations of strain at each sites.

beginning of the recording session, and strain gauges were periodically re-balanced when the animal was not eating. While chewing, the animals were videoed in frontal view with a SONY DCRVX-1000 digital camera (SONY, New York, NY) at 60 Hz with a small diode light in the corner of the field of view synchronized to a 1 V signal recorded on the tape recorder. Animals were re-recorded between 3 and 24 hours following surgery.

Following the second recording, each animal was anaesthetized as described above; sutures were removed, the gauges exposed and the orientations of the A-elements re-measured. Gauges were then removed, the incision site cleaned and re-sutured, and the animal allowed to recover.

Waveform analysis

Strain data from long chewing sequences of different foods were sampled from the tape recorder on a Macintosh G4 computer using an Ionet™ A-D board (GW Instruments, Somerville MA) at 250 Hz. A Superscope 3.0™ (GW Instruments, Somerville MA) virtual instrument (written by DEL) was used to determine the zero offset, calculate strains in microstrain units ($\mu\varepsilon$) of principal tension (ε_1) and compression (ε_2) from raw voltage data using shunt calibration signals recorded during the experiments, and calculate the orientation of principal tension in degrees relative to the A-element of each gauge ($\varepsilon_1°$) using formulae from Biewener (1992). All waveform data were output to Igor Pro v. 3.01 (Wavemetrics Inc., Lake Oswego, NY) for visualization and analysis. An IGOR macro was used to measure peak ε_1, ε_2, $\varepsilon_1°$ and shear (γ, calculated as $\varepsilon_1 - \varepsilon_2$) for a minimum of 20 strokes on the active and balancing side for each food type for each animal (in a few cases, fewer than 20 chews were available). Side of chew was determined by using selected sequences in which synchronized video recordings of the animal were related to patterns of strain as well as the relative timing of contractions of the posterior *m. temporalis*, which continues to contract on the balancing side after cessation of activity on the working side. For these sequences, data were analyzed at 5,000 Hz.

Morphometric measurements and analysis

Computed tomography (CT) scans were taken of the hard and soft treatment group animals at

the beginning and end of the treatment period using a GE Medical Scanner. Animals were sedated prior to scanning with Ketamine (0.2 mg/kg), Xylazine (1.0 mg/kg) and Atropine (0.04 mg/kg). Slice thickness was 1.0 mm. Twenty-four cranial and ten mandibular landmarks (listed in Table 1) were collected from each scan using ETDIPS (www.cc.nih.gov/cip/software/etdips/). Cranial landmarks were selected with an emphasis on primary sites of growth in the lower face, especially sutures. Measurement error in landmarking was analyzed by comparing caliper measurements of the linear distances between a subset of 13 landmarks on a single cranium with the mean of the inter-landmark distances obtained from a CT scan of the same cranium; this procedure was repeated five times. The error measurement for the inter-landmark distances, compared to the mean of the caliper measurements, ranged from 0.2–9.0% (0.3–1.7 mm), mean=4.31%. Unfortunately, it is difficult to define landmarks to quantify accurately the height and thickness of the mandibular corpus and symphysis. Consequently, linear caliper measurements of maximum corpus width and height at M_1, and maximum height and width of the symphysis were taken *post-mortem* in each animal.

The three dimensional landmark coordinate data were analyzed using Euclidean Distance Matrix Analysis (EDMA) to assess the influence of experimental treatment on facial shape and growth. EDMA analyzes all possible linear inter-landmark distances without reference to a coordinate system to quantify differences in both form and growth between samples (Lele and Richtsmeier, 1991; Lele, 1993). Form matrices for each individual were first calculated as the Euclidean distance matrix of all inter-landmark distances, and then scaled by the geometric mean of all inter-landmark distances to compare facial shape. WinEDMA software (http://oshima.la.psu.edu/jrlab/adm/edma.html) was used in for all analyses. Form difference matrices (FDM) were then calculated as the ratio of like linear distances between samples. To compare longitudinal 3D facial growth between hard and soft food treatment groups, growth difference matrices (Richtsmeier and Lele, 1993) were calculated as the

Table 1
Three-dimensional landmarks used

CRANIAL
1 Nasion
2 Nasospinale
3 Rhinion
4 Most lateral point on coronal suture at intersection with orbital rim, right
5 Most lateral point on coronal suture at intersection with orbital rim, left
6 Most dorsal point on zygomaticomaxillary suture (zygomaxillare superior), right
7 Most dorsal point on zygomaticomaxillary suture (zygomaxillare superior), left
8 Right maxillary tuberosity
9 Left maxillary tuberosity
10 Right midrostral point (intersection of nasal/maxilla/premaxilla sutures)
11 Left midrostral point (intersection of nasal/maxilla/premaxilla sutures)
12 Midpalatal suture (intersection of palatomaxillary and midpalatal sutures)
13 Right inferior maxilla (lowest lateral point on right maxilla between M^1 and M^2)
14 Left inferior maxilla (lowest lateral point on left maxilla between M^1 and M^2)
15 Basion
16 External occipital protuberance (EOP)
17 Opisthion
18 Bregma
19 Most ventral point on zygomaticomaxillary suture (zygomaxillare inferior), right
20 Most ventral point on zygomaticomaxillary suture (zygomaxillare inferior), left
21 Right maxilla at P^3 (suture anterior to right first premolar)
22 Left maxilla at P^3 (suture anterior to left first premolar)
23 Right zygomatico-temporal suture, most dorsal point
24 Left zygomatico-temporal suture, most dorsal point

MANDIBULAR
1 Infradentale superior
2 Right condylion laterale
3 Left condylion laterale
4 Right gonion
5 Left gonion
6 Gnathion
7 Right superior mandible (right highest lateral point on mandible between M_1 and M_2)
8 Left superior mandible (left highest lateral point on mandible between M_1 and M_2)
9 Right inferior mandible (right lowest lateral point on mandible between M_1 and M_2)
10 Left inferior mandible (left lowest lateral point on mandible between M_1 and M_2)

Table 2
In vivo strains from the zygomatic arch (left side)

Food	Side	Animal	*N*	Tension, ε_1	Compression, ε_2	Shear, γ_{max}	Angle*	$\varepsilon_1/\lvert\varepsilon_2\rvert$
soft carrot	W (left)	H1 (6/'00)	23	193 (310)	−137 (18)	329 (48)	−80.96 (2.87)	1.41 (0.12)
soft carrot	B (right)	H1 (6/'00)	15	109 (20)	−58 (20)^{B}	167 (37)^{B}	−77.49 (7.36)	2.05 (0.67)
dry apple	W (left)	H1 (6/'00)	123	891 (156)	−838 (178)	1729 (300)	−79.41 (3.30)	1.09 (0.20)
dry apple	B (right)	H1 (6/'00)	18	570 (83)^{B}	−499 (87)^{B}	1069 (93)^{B}	−79.16 (3.59)	1.18 (0.29)
soft apple	W (left)	H1 (6/'00)	14	352 (121)^{S}	−283 (94)^{S}	635 (215)^{S}	−79.57 (2.49)	1.24 (0.06)
soft apple	B (right)	H1 (6/'00)	22	163 (17)^{S,B}	−147 (21)^{S,B}	310 (37)^{S,B}	−87.17 (4.92)	1.12 (0.09)
kale	W (left)	H3 (10/'00)	77	421 (85)	−275 (76)	696 (160)	−76.52 (2.77)	1.56 (0.14)
kale	B (right)	H3 (10/'00)	35	199 (42)^{B}	−126 (28)^{B}	325 (69)^{B}	−80.44 (4.05)	1.60 (0.11)
dry carrot	W (left)	H3 (10/'00)	27	460 (77)	−305 (62)	765 (137)	−79.10 (2.40)	1.52 (0.12)
dry carrot	B (right)	H3 (10/'00)	27	176 (42)^{B}	−136 (26)^{B}	312 (67)^{B}	−82.36 (3.40)	1.29 (0.11)
soft apple	W (left)	H3 (10/'00)	8	281 (78)	−206(60)^{S}	487 (138)^{S}	−79.93 (2.08)	1.37 (0.07)
soft apple	B (right)	H3 (10/'00)	32	155 (31)^{S,B}	−114 (25)^{S}	270 (56)^{S,B}	−81.28 (1.50)	1.36 (0.07)
dry apple	W (left)	H3 (10/'00)	33	510 (93)	−356 (86)	866 (175)	−77.31 (1.72)	1.45 (0.09)
dry apple	B (right)	H3 (10/'00)	3	295 (130)^{B}	−201 (107)	495 (237)^{B}	−76.70 (1.14)	1.43 (0.002)
Mean hard food	W		4	570.50	−443.50	1014.00	−78.09	1.41
Mean hard food	B		4	310.00	−240.50	550.25	−79.67	1.38
Mean soft food	W		3	275.33	−208.67	483.67	−80.15	1.34
Mean soft food	B		3	142.33	−106.33	249.00	−81.98	1.51

Values in parentheses are standard deviations.
*Angle relative to the coronal plane.
^{B}Strain values (within individuals) for balancing side significantly different ($p<0.05$) from working side (ANOVA).
^{S}Strain values (within individuals) for soft food significantly different ($p<0.05$) from hard food (ANOVA).

mean ratio of like linear distances (scaled by each individual's overall size) of the mean FDMs for the hard versus soft food treatment groups at the end versus beginning of the treatment period. Ratios different from 1.0 indicate inter-landmark distances in which more or less growth has occurred in one of the samples. Significant differences between hard and soft food treatment groups for each linear distance were tested using 1000 bootstraps with replacement to compute 90% confidence intervals (α=0.10; p=0.10) (Lele and Richtsmeier, 1991, 1995). Note that confidence intervals were calculated using 1,000 bootstrap analyses for each interlandmark ratio separately. Two-tailed test of significance were used to avoid making a priori assumptions of which interlandmark distances would be relatively larger or smaller. We report only results for which the 90% confidence interval is <1.0 or >1.0, and include the confidence intervals in Tables 8 and 9.

Results

Strain gauge analysis

Tables 2–7 summarize means and standard deviations for in vivo peak strains calculated from multiple chews (peak ε_1, ε_2, γ, ε_1°, and $\varepsilon_1/\varepsilon_2$) by gauge location and food type for each subject, with two individuals for most gauge locations. Ranges are not included to save space, but may be obtained from the authors. Figure 4 illustrates the orientations of principal strains for each location. In one experiment, one individual (Hyrax 2, 10/'00), chewed only on the right side (hence only left side data are presented). In addition, strain values for soft food were not recorded in all experiments, preventing comparison of strain magnitudes for soft and raw/dried (hereafter referred to as hard) food for the interorbital region and the dorsal rostrum.

Table 3
In vivo strains in the mandibular corpus

Food	Side	Animal	*N*	Tension, ε_1	Compression, ε_2	Shear, γ_{max}	Angle*	$\varepsilon_1/\lvert\varepsilon_2\rvert$
dry apple	W (left)	H3 (7/'00)	29	186 (44)	−495 (120)	681 (162)	81.92 (5.25)	0.38 (0.03)
dry apple	B (left)	H3 (7/'00)	33	271 (63)[B]	−651 (132)	922 (182)[B]	4.05 (4.13)[B]	0.42 (0.07)
soft apple	W (left)	H3 (7/'00)	23	194 (37)	−508 (92)	702 (128)	78.04 (6.42)	0.38 (0.02)
soft apple	B (left)	H3 (7/'00)	5	163 (26)[S]	−424 (33)[B]	587 (58)[S]	6.05 (1.46)[B]	0.38 (0.03)
soft carrot	W (left)	H3 (7/'00)	28	137 (50)	−427 (138)	564 (185)	82.93 (6.86)	0.32 (0.04)
soft carrot	B (left)	H3 (7/'00)	20	206 (122)	−564 (292)	770 (413)	5.56 (3.56)[B]	0.36 (0.04)
kale	W (left)	H3 (7/'00)	18	274 (19)	−727 (44)	1001 (61)	85.85 (5.43)	0.38 (0.02)
kale	B (left)	H3 (7/'00)	7	337 (51)[B]	−757 (78)	1093 (119)	5.54 (3.81)[B]	0.44 (0.05)
sweet potato	W (right)	H2 (10/'00)	31	122 (31)	−253 (66)	374 (96)	−82.06 (2.04)	0.46 (0.05)
dry apple	W (right)	H2 (10/'00)	36	111 (35)	−222 (74)	333 (110)	−82.81 (1.51)	0.51 (0.04)
dry carrot	W (right)	H2 (10/'00)	39	125 (26)	−283 (61)	408 (86)	−82.56 (1.18)	0.45 (0.03)
Mean hard food	B		2	304	−704	1008	4.8	0.43
Mean hard food	W		5	218	−396	559	83.6	0.44
Mean soft food	B		2	184	−494	679	5.8	0.37
Mean soft food	W		2	166	−468	633	80.5	0.35

Values in parentheses are standard deviations.
*Angle relative to the coronal plane.
[B]Strain values (within individuals) for balancing side significantly different ($p<0.05$) from working side (ANOVA).
[S]Strain values (within individuals) for soft food significantly different ($p<0.05$) from hard food (ANOVA).

Table 4
In vivo strains in the mandibular symphysis

Food	Side	Animal	*N*	Tension, ε_1	Compression, ε_2	Shear, γ_{max}	Angle*	$\varepsilon_1/\lvert\varepsilon_2\rvert$
dry apple	B (left)	H3 (7/'02)	62	211 (51)	−457 (101)	667 (151)	39.03 (3.0)	0.46 (0.04)
soft apple	B (left)	H3 (7/'02)	28	178 (34)	−407 (94)	595 (137)	38.71 (1.14)	0.44 (0.01)
soft carrot	B (left)	H3 (7/'02)	48	175 (77)	−487 (208)	691 (279)	37.91 (7.2)	0.43 (0.07)
kale	B (left)	H3 (7/'02)	25	284 (36)	−596 (81)	879 (117)	39.25 (2.35)	0.48 (0.01)
sweet potato	W (left)	H2 (10/'00)	31	239 (160)	−470 (120)	709 (239)	−43.63 (20.21)	0.49 (0.25)
dry apple	W (left)	H2 (10/'00)	36	246 (159)	−385 (130)	632 (261)	−34.52 (21.98)	0.64 (0.32)
dry carrot	W (left)	H2 (10/'00)	39	181 (84)	−492 (150)	673 (218)	−46.39 (11.44)	0.37 (0.12)
Mean hard food	B		2	245	−464	688	36.7	0.55
Mean hard food	W		5	222	−449	671	−41.5	0.50
Mean soft food	B		2	177	−447	643	38.3	0.44
Mean soft food	W		0	na	na	na	na	na

Values in parentheses are standard deviations.
*Relative to sagittal plane; NB H3 is a right side symphysis; H2 is a left side symphysis (hence opposite signs for angles).

Strain differences between hard and cooked foods do not vary in terms of strain orientation or mode ($\varepsilon_1/\varepsilon_2$) at any site, but they do vary in magnitude at several sites. In the zygomatic arch (Table 2), which is pulled ventrally by the masseter, strains are approximately twice as high for hard versus cooked foods, but with no significant difference in angle or mode. Working side strains are also approximately twice the magnitude of balancing side strains for all food types.

Table 5
In vivo strains from on the anterior dorsal rostrum (left of midline)

Food	Side	Animal	*N*	Tension, ε_1	Compression, ε_2	Shear, γ_{max}	Angle*	$\varepsilon_1/\lvert\varepsilon_2\rvert$
raw carrot	W (left)	H3 (3/'02)	13	43 (18)	−113 (55)	156 (74)	−49.85 (1.18)	0.39 (0.05)
raw carrot	B (right)	H3 (3/'02)	50	34 (13)	−18 (8)[B]	52 (21)[B]	54.17 (3.79)[B]	2.00 (0.34)[B]
raw lettuce	W (left)	H3 (3/'02)	29	32 (9)	−104 (28)	136 (36)	−50.16 (2.07)	0.31 (0.03)
raw lettuce	B (right)	H3 (3/'02)	20	19 (7)[B]	−16 (4)[B]	35 (11)[B]	48.44 (20.21)[B]	1.11 (0.17)[B]
raw apple	W (left)	H3 (3/'02)	4	35 (24)	−102 (79)	137 (103)	−48.00 (10.60)	0.38 (0.06)
raw apple	B (right)	H3 (3/'02)	6	24 (3)	−14 (1)[B]	38 (3)[B]	32.38 (5.34)[B]	1.69 (0.28)[B]
Mean hard food	W		6	37	−106	143	−49.3	0.36
Mean hard food	B		6	27	−16	43	44.9	1.60

Values in parentheses are standard deviations.
*Angle relative to the sagittal plane.
[B]Strain values (within individuals) for balancing side significantly different ($p<0.05$) from working side (ANOVA).

Table 6
In vivo strains in interorbital region (left of midline)

Food	Side	Animal	*N*	Tension, ε_1	Compression, ε_2	Shear, γ_{max}	Angle*	$\varepsilon_1/\lvert\varepsilon_2\rvert$
raw carrot	B (right)	H2 (2/'02)	34	126 (45)[B]	−74 (31)	200 (74)	14.81 (2.50)[B]	1.76 (0.30)[B]
raw carrot	W (left)	H2 (2/'02)	12	53 (17)	−102 (42)	155 (58)	−79.90 (1.40)	0.54 (0.12)
raw potato	B (right)	H2 (2/'02)	30	273 (64)[B]	−159 (44)	432 (107)[B]	13.03 (0.36)[B]	1.74 (0.11)[B]
raw potato	W (left)	H2 (2/'02)	35	57 (11)	−151 (34)	208 (42)	−76.17 (1.99)	0.39 (0.07)
raw apple	B (right)	H2 (2/'02)	32	254 (113)[B]	−140 (68)[B]	394 (180)[B]	12.87 (0.65)[B]	1.86 (0.19)[B]
raw apple	W (left)	H2 (2/'02)	13	40 (9)	−99 (21)	139 (16)	−76.28 (3.18)	0.42 (0.19)
raw carrot	W (left)	H3 (3/'02)	67	150 (86)	−35 (11)	186 (92)	−45.85 (2.57)	4.52 (2.28)
raw carrot	B (right)	H3 (3/'02)	13	16 (5)[B]	−231 (62)[B]	247 (67)	48.60 (0.98)[B]	0.07 (0.01)[B]
raw lettuce	W (left)	H3 (3/'02)	46	166 (58)	−28 (8)	194 (62)	−44.57 (1.60)	5.82 (1.89)
raw lettuce	B (right)	H3 (3/'02)	29	21 (3)[B]	−193 (23)[B]	214 (26)	49.19 (0.53)[B]	0.11 (0.007)[B]
raw apple	W (left)	H3 (3/'02)	10	107 (42)	−34 (6)	140 (46)	−46.36 (2.24)	3.17 (1.18)
raw apple	B (right)	H3 (3/'02)	4	10 (2)[B]	−138 (33)[B]	147 (34)	45.89 (2.47)[B]	0.07 (0.02)[B]
Mean hard food	W		6	96	−75	170	−45.0	2.48
Mean hard food	B		6	117	−156	272	47.2	0.94

Values in parentheses are standard deviations.
*Angle relative to the sagittal plane.
[B]Strain values (within individuals) for balancing side significantly different ($p<0.05$) from working side (ANOVA).

Differences in strains generated by masticating hard versus cooked food are less extreme in the mandible. In the mandibular corpus (Table 3), mastication of hard foods generate approximately 48% higher shear strains on the balancing side, but approximately equal shear strains on the working side; in the symphysis (Table 4), hard foods generate only slightly but not significantly higher balancing side shear strains. Strain orientations in the mandible do not differ with food hardness, but $\varepsilon_1/\varepsilon_2$ ratios are slightly lower for cooked foods, reflecting relatively more compression. Unfortunately, no cooked food strain data were recorded for the dorsal rostrum (which experienced extremely low strains) or the interorbital region (which experienced moderately low strains). Further experiments are needed, but two results suggest a likelihood of some difference in strain

Table 7
In vivo strains on metopic suture (interorbit)

Food	Side	Animal	*N*	Tension, ε_1	Compression, ε_2	Shear, γ_{max}	Angle*	$\varepsilon_1/\lvert\varepsilon_2\rvert$
kale	l	H3 (10/'00)	77	960 (167)	−785 (134)	1744 (256)	−45.91 (0.76)	1.23 (0.10)
kale	r	H3 (10/'00)	35	927 (121)	−1390 (290)[B]	2317 (472)	44.10 (1.1)[B]	0.67 (0.10)[B]
dry carrot	l	H3 (10/'00)	27	1105 (250)	−962 (184)	2067 (428)	−42.22 (2.10)	1.15 (0.09)
dry carrot	r	H3 (10/'00)	27	983 (312)	−1397 (459)	2380 (761)	44.17 (1.86)[B]	0.71 (0.08)[B]
soft apple	l	H3 (10/'00)	8	467 (292)	−346 (253)[S]	813 (544)[S]	−50.69 (3.78)	1.42 (0.26)
soft apple	r	H3 (10/'00)	32	496 (238)	−640 (402)	1136 (637)	47.26 (5.94)[B]	0.86 (0.27)[B]
dry apple	l	H3 (10/'00)	33	850 (169)	−677 (140)	1517 (304)	−41.96 (1.76)	1.28 (0.09)
dry apple	r	H3 (10/'00)	3	349 (60)	−812 (61)	1160 (121)	39.03 (3.81)[B]	0.43 (0.04)[B]
Mean hard food	L		4	845.5	−692.5	1535.25	−45.195	1.27
Mean hard food	R		4	688.75	−1059.75	1748.25	43.64	0.6675

Values in parentheses are standard deviations.
*Angle relative to the sagittal plane.
[B]Strain values within individuals for left and right sides significantly different ($p<0.05$; ANOVA).
[S]Strain values (within individuals) for soft food significantly different ($p<0.05$) from hard food (ANOVA).

magnitude between hard versus cooked foods in the interorbital region. First, interorbital strains generated by chewing different foods vary substantially (e.g., strains from chewing raw potato are approximately twice that for carrot). Second, strains in the metopic suture (Table 7) generated by masticating hard food are approximately twice that of cooked food.

Tables 2–7 indicate that strain magnitudes differ considerably between locations, with evidence for a gradient of strains relative to the occlusal plane or sites of muscle origin/insertion. Considering only hard foods (for which data exist for all locations), mean shear values (γ) in the mandible are approximately 600–1000 με in the corpus, and 600–800 με in the symphysis; mean shear values in the working side zygomatic are similarly high (approximately 1000 με). In contrast, working and balancing side strains during mastication of hard foods are moderate in the interorbital region (170 με), and very low (50 με) in the dorsal rostrum.

Analyses of principal strain orientation (summarized in Fig. 4) indicate a complex picture. The zygomatic arch is always bent approximately perpendicular relative to the coronal plane (Table 2) regardless of side or food type as a result of the ventrally-directed force of the masseter. Orientation of principal strain in the mandibular corpus (Table 3) is approximately vertical (in the coronal plane) during balancing side mastication, and shifts almost 90° to horizontal (aligned with the sagittal plane) during working side mastication, consistent with a pattern of strain dominated by bending in the sagittal plane. Orientation of principal strain in the symphysis (Table 4) is approximately 45° relative to sagittal plane during both working and balancing side chews with an approximately 90° change across side-shifts, consistent with a strain regime dominated by dorsoventral shear (Hylander, 1984). The 45° orientation of ε_1°, however, could also result from twisting of the balancing side corpus around a longitudinal axis and/or from lateral transverse bending (see below).

The patterns of strain orientation in the rostrum (Table 5) and interorbital (Table 6) regions differ from those documented in the mandible and zygomatic arch. Principal strain orientations in both regions are approximately 45° relative to the sagittal plane in the expected orientation of twisting (towards the balancing side), with 90° shifts from working to balancing side. However in one animal (H2, 2/02) working and balancing side angles in the interorbital region consistently differ in predicted orientation by approximately 30°. In addition, strain mode shifts considerably between balancing and working side chews, with high ratios

Table 8
Form difference matrix analysis results (numbers match distances in Fig. 5)

		Ratio		
	No.	% (HD/SD)	(HD/SD)	Confidence interval
Dimensions of posterior face/neurocranium significantly larger in hard diet group				
Posterior zygomatic—EOP	1	14.1	1.141	1.015–1.265
Posterior zygomatic—basion	2	13.3	1.133	1.068–1.202
Posterior zygomatic—opisthion	3	12.8	1.128	1.034–1.226
Basion—EOP	4	7.5	1.075	1.043–1.105
Frontal/zygomatic junction—basion	5	5.5	1.055	1.013–1.099
Maxillary tuberosity—EOP	6	5.4	1.054	1.013–1.091
Maxillary tuberosity—EOP	6	4.5	1.045	1.001–1.083
Maxillary tuberosity—contralateral posterior zygomatic	7	3.2	1.032	1.006–1.064
Zygomaxillare superior—basion	8	2.7	1.027	1.001–1.056
Dimensions of posterior face/neurocranium significantly smaller in hard diet group				
Nasion—posterior diastema	9	−7.4	0.926	0.888–0.959
Maxilla at P3—ipsilateral posterior zygomatic	10	−7.1	0.929	0.883–0.978
Midrostral point—ipsilateral posterior zygomatic	11	−6.3	0.937	0.880–0.991
Midpalatal suture—inferior zygomatic	12	−5.7	0.943	0.893–0.996
Maxilla at P3—contralateral posterior zygomatic	13	−4.9	0.951	0.909–0.991
Midrostral point—contralateral posterior zygomatic	14	−4.7	0.953	0.915–0.990
Nasion—posterior zygomatic	15	−4.1	0.953	0.911–0.993
Nasion—inferior zygomatic	16	−3.6	0.959	0.924–0.992
Dimensions of anterior face significantly larger in hard diet group				
Left midrostral point—right maxilla at P3	17	9.8	1.098	1.011–1.188
Nasale—midpalatal suture	18	7.1	1.071	1.013–1.126
Right inferior zygomatic—left midrostral point	19	5.3	1.053	1.028–1.080
Right inferior zygomatic—nasale	20	5.2	1.052	1.001–1.104
Right inferior zygomatic—left inferior maxilla	21	3.9	1.039	1.009–1.070
Right inferior zygomatic—left zygomaxillare superior	22	3.0	1.030	1.005–1.056
Dimensions of anterior face significantly smaller in hard diet group				
Nasion—bregma	23	−11.3	0.887	0.798–0.972
Left zygomaxillare superior—bregma	24	−6.1	0.939	0.883–0.996
Right frontal/zygomatic junction—right maxilla at P3	25	−4.7	0.953	0.917–0.995
Opisthion—right maxilla at P3	26	−3.0	0.970	0.941–0.999

(>1.0) of tensile to compressive strain on the balancing side, and low ratios (<1.0) on the working side. Comparison of Tables 6 and 7 indicate that strains recorded on the metopic suture differ from those measured just lateral to the suture primarily in terms of magnitude (mean shear values on the suture are 1,641 με, approximately six times as high) and the ratio of tension/compression (which range from 0.7–1.4), but not in terms of angle, which also indicates twisting.

Form and growth difference analyses

Table 8 summarizes and Fig. 5 illustrates results of the form difference analysis comparing hard versus soft diet treatment groups at the end of the treatment period. Only interlandmark differences significant at the α=0.10 level are listed. As one might expect for an experiment of only 100 days, there are no major differences in overall cranial shape between the groups, but several

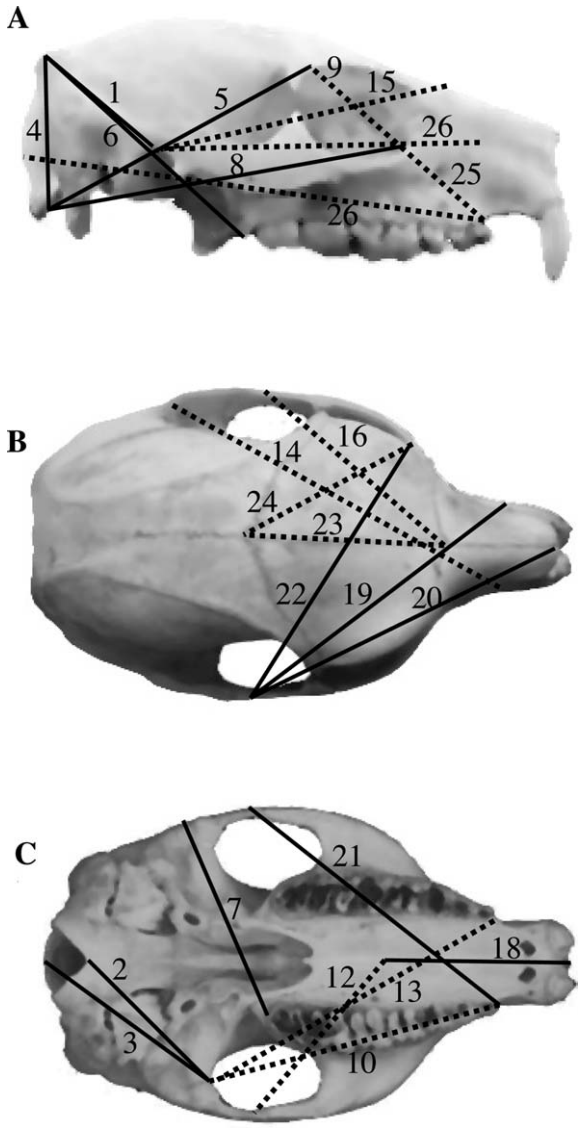

Fig. 5. Results of EDMA form difference matrix analysis of hyraxes fed hard versus soft food. Details of analysis are summarized in the text. Solid lines are inter-landmark distances (scaled by the geometric mean of all interlandmark distances) significantly longer in the hard food group; dashed lines are inter-landmark distances (scaled by the geometric mean of all interlandmark distances) significantly longer in the soft food group. Numbers indicate dimensions in Table 8.

interlandmark dimensions are significantly different in relative length between the hard- and soft-diet groups, especially in the ventral and posterior portions of the face, and the neurocranium. In particular, size-adjusted distances between the posterior zygomatic arch and landmarks on the posterior and inferior aspects of the cranium (external occipital protuberance, basion and opisthion) are 12–14% greater in the hard diet group; in addition, in the hard diet group the distance from the maxillary tuberosity is approximately 5% longer to the external occipital protuberance and 3.2% greater to the zygomatic arch. Several differences in shape are also evident in the anterior, rostral portion of the face. Notably, interlandmark distances between the lower maxilla (e.g., the midrostral point, nasale, the inferior maxilla) and the contralateral zygomatic arch are significantly longer, and the rostrum is both wider (midrostral point—right maxilla at P^3) and taller (nasale—midpalatal suture).

In the analysis of cranofacial shape, some interlandmark distances were smaller in the hard diet group than in the soft diet group, particularly in the dorsal and rostral portions of the cranium. Such a pattern is evident from Table 8 and Fig. 4. For example, the distance from nasion to bregma is 11.3% smaller, and the distance from nasion to the landmarks on the zygomatic arches is 3.6–7.4% smaller in the hard diet group. In addition, the distance between the back of the face and several points on the anterior rostrum tend to be relatively smaller in the hard diet group.

Table 9 summarizes and Fig. 6 illustrates the results of the scaled growth difference comparisons between the hard and soft diet treatment groups that occurred during the treatment period. Only interlandmark differences significant at the α=0.10 level are listed. In general, differences in growth between the treatment groups reflect the differences in shape noted above, except that there are no landmarks for which significantly less growth occurred in the hard diet group. In particular, the hard diet group had more mediolateral and anteroposterior growth (16–17%) between the zygomatic arches and points on the posterior and inferior aspects of the cranial vault (e.g., basion, opisthion, external occipital protuberance), and 7.5–8.5% more growth between the maxillary tuberosities and points on the neurocranium. The hard diet group also had more anteroposterior growth (7–8%) between the zygomatic arch and landmarks

Table 9
Growth difference matrix analysis results (scaled). (Numbers match distances in Fig. 6)

		Ratio		
	No.	% (HD/SD)	(HD/SD)	Confidence interval
Anterior facial dimensions with significantly more growth in hard diet group				
Midrostral point—contralateral inferior zygomatic	1	8.1	1.081	1.003–1.166
Inferior maxilla—contralateral inferior zygomatic	2	6.8	1.068	1.009–1.133
Posterior face/neurocranium dimensions with significantly more growth in hard diet group				
Posterior zygomatic—EOP	3	17.1	1.171	1.003–1.369
Posterior zygomatic—basion	4	16.5	1.165	1.046–1.304
Posterior zygomatic—opisthion	5	15.9	1.159	1.027–1.310
Posterior zygomatic—contralateral maxillary tuberosity	6	6.1	1.061	1.005–1.124
Maxillary tuberosity—EOP	7	7.5	1.075	1.016–1.129
Maxillary tuberosity—EOP	8	8.5	1.085	1.026–1.139
Basion—Bregma	9	7.6	1.076	1.010–1.144
Basion—EOP	10	10.5	1.105	1.022–1.183

on the maxilla and rostrum. Many of the significant differences in growth are between posterolateral and anteromedial landmarks of the midface and maxilla (see below).

The growth difference analysis revealed no significant differences in the growth of mandibular dimensions between landmarks identified on the hard and soft diet groups, possibly due to fewer biologically relevant landmarks on the mandible. However, linear caliper measurements taken directly on the mandibles and standardized by mandibular length indicate 15% greater corpus height and 14% greater corpus thickness in the hard diet group at M_1 ($p<0.03$, Mann–Whitney U test). Relative height and thickness of the symphysis, however, was not significantly different between the two groups.

Discussion

The above results support the general hypothesis that human faces may have become relatively smaller despite increases in body size because of reduced levels of strain generated by chewing softer, more processed food. This hypothesis was divided into several more specific hypotheses about strain and growth. The first strain hypothesis, that soft, cooked foods generate less strain than hard, uncooked foods, was partially supported, although the picture is somewhat complex. In particular, in the zygomatic arch, strain generated by hard food is approximately twice that of cooked food, particularly on the balancing side; balancing but not working side mandibular corpus strains are also about twice as high when chewing hard food. Interestingly, symphysis strains did not differ significantly between hard versus soft foods, and strain differences are less marked in regions with lower strain magnitudes such as the interorbital and the rostrum. These results need to be corroborated with further experiments. Differences between balancing and the working side strains presumably result from less recruitment of balancing side adductor force when chewing softer foods (a hypothesis that requires further testing with EMG data). One important point to note is that the above data compare strains generated by masticating desiccated versus microwaved food rather than hard food with completely softened, nearly liquid food. In such cases, differences in strain are even greater, approximately by an order of a magnitude (Lieberman et al., unpublished data).

The above data also support the second strain hypothesis, that the pattern of strains in the hyrax face follows a gradient in which strains are higher near the sites of occlusion and muscle insertion and dissipate dorsally away from the tooth row. In the hyrax, strain magnitudes are several times higher in the mandible and in the zygomatic arch

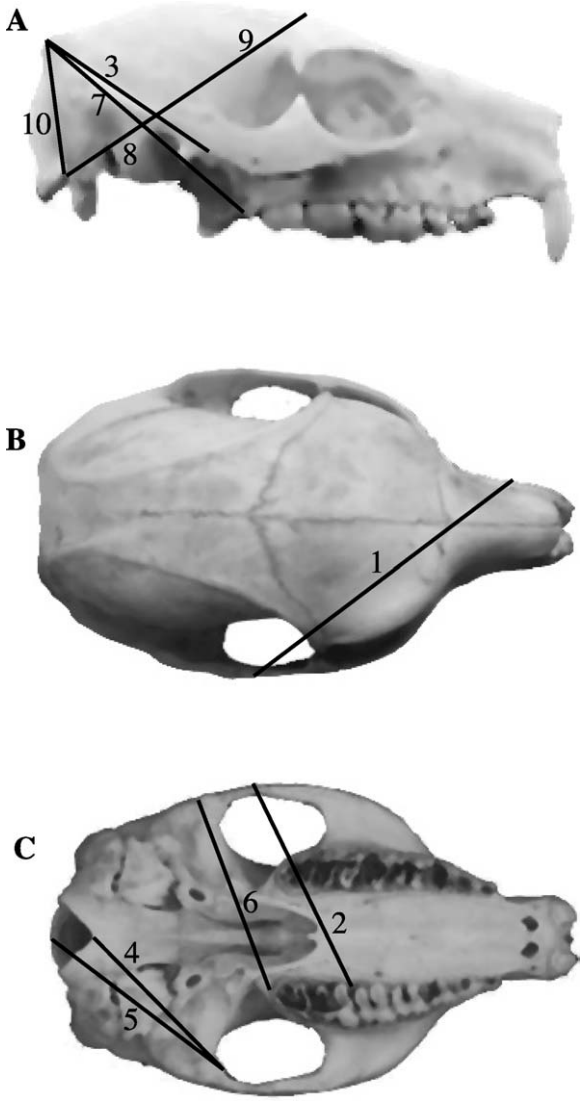

Fig. 6. Results of EDMA growth difference matrix analysis of hyraxes fed hard versus soft food. Details of analysis are summarized in the text. Lines are inter-landmark dimensions in which significantly more growth occurred in the hard versus soft food hyrax treatment group. Numbers indicate dimensions in Table 8. There were no inter-landmark distances in which significantly more growth occurred in the soft food hyrax treatment group.

than in the top of the skull, resembling the gradient documented in several species of non-human primates (Hylander et al., 1991a; Hylander and Johnson, 1992; Hylander and Ravosa, 1992; Ross and Hylander, 1996; Ravosa et al., 2000b). It is possible that the facial gradient is a little steeper in hyraxes than in non-human primates. In macaques and baboons, strains in the infraorbital and zygomatic regions are about 2.8 times higher than in the interorbital region, and about 5.8 times higher than in the dorsal interorbital region (Hylander et al., 1991a; Hylander and Johnson, 1992). Although gauge locations in the hyrax are slightly different, working side strains in the zygomatic arch during hard food mastication are about six times higher than in the interorbital region, and about seven times higher than in the dorsal rostrum. Although the morphological and biomechanical bases for strain gradients are not well understood, it is interesting to note that the hyrax pattern is more similar to non-human primates than to miniswine (Herring et al., 2001), which are even more prognathic than primates and have an apparently much steeper strain gradient. For example, in miniswine, shear strain in the zygomatic arch is about twice that of strain in the dorsal rostrum (the maxillary bone) but approximately ten times higher than in the interorbital frontal (Herring and Mucci, 1991; Rafferty and Herring, 1999; Herring et al., 2001). More precise comparisons of strain gradients in hyraxes and other species, however, will require more data on more functionally comparable locations from multiple species, and from additional subjects.

There are also some interesting similarities and differences in terms of the pattern of strain orientation in the hyrax compared to the pattern documented in various non-human primates and other mammals. As noted above, the general pattern of strain in the hyrax mandibular corpus appears to be somewhat similar to non-human primates (Hylander, 1979; Hylander et al., 1987) as well as miniswine (Herring et al., 2001), with predominantly sagittal bending; in addition, the pattern of strain in the hyrax symphysis corresponds best either to dorso-ventral shearing or to a combination of wishboning and twisting—not unlike the pattern documented in non-human anthropoids (Hylander, 1984; Hylander and Johnson, 1992). However, additional data from more subjects as well as other gauge positions are necessary to distinguish between these different

possibilities. For example, the highly transverse nature of the hyrax power stroke in combination with the lateral orientation of the deep masseter suggest that wishboning is likely to occur, but further studies are necessary with larger sample sizes, EMG data, and gauges on the dorsal and ventral margins of the symphysis.

Perhaps the most interesting but puzzling difference between the hyrax and some non-human primates is the predominance of twisting evident in the rostrum and interorbital region in the hyrax. In gauges mounted on the metopic suture, just off the midline in the interorbital region, and on the rostrum, the angle of principal strain in the hyrax is generally close to 45° to the long axis of the cranium in the direction of occlusion, and changes 90° with side shifts. This pattern has been documented in swine (Herring and Teng, 2000), and non-anthropoids such as *Otolemur* by Ravosa et al. (2000a,b), but not consistently in non-human anthropoids which appear to be somewhat variable in this regard (Hylander et al., 1991a,b; Ross and Hylander, 1996; Ross, 2001). There are several possibilities for this similarity to strepsirrhines, as well as to some anthropoids (see Ross, 2001). One possibility may be related to retrognathy. As noted above, the rostrum probably withstands much of the twisting stress generated by unilateral occlusion in animals whose teeth lie beneath a rostrum in front of the orbital plane. In contrast, stresses may be greater in the orbital region in retrognathic mammals in which strains cannot be dissipated substantially in the rostrum. This hypothesis seems unlikely, however, given the substantial retrognathy in *Aotus*, which do no show strong evidence for twisting (Ross and Hylander, 1996). Alternatively, twisting in the hyrax skull may be a function of its generally narrow, tubular shape in which little mass is distributed far from the skull's long axis. Finally, twisting of the orbital region is also influenced by the relative proportion of working side to balancing side (W/B) adductor muscle force, which has been estimated to be substantially higher in strepsirrhines than anthropoids based on EMG activity ratios (Hylander et al., 2000). However, judging from the high ratio of W/B strains in the zygomatic arch, the hyrax probably has high W/B adductor ratios that will generate less torque, leading to less twisting. In order to test this hypothesis, data on W/B adductor force ratios are needed for the hyrax.

In short, the pattern of deformation documented in the hyrax face is mostly consistent with twisting in the face, bending in the zygomatic arch, and a combination of sagittal and lateral transverse bending in the mandibular corpus in which strains decline steeply from the region of occlusion to the upper face (note that the high strains in the metopic suture do not disprove the existence of the strain gradient described here for facial bones; strains are always higher in sutures than in bones [Herring and Teng, 2000]). In addition, strains generated by masticating hard food are typically higher than those generated by masticating cooked food. Regardless of what aspects of facial shape and muscle recruitment cause this pattern, these strains are predicted to influence facial growth in animals raised on different diets. In particular, we tested three growth hypotheses: animals raised on harder, uncooked foods were predicted to have more facial growth than animals raised on softer, more processed foods; variations in regional growth were predicted to correlate with regional strain; and growth is predicted to occur in the plane of deformation. The experiment reported here examined only a short period of growth (98 days) in a tiny sample. Nevertheless, the results are significant with respect to all three hypotheses. The hyraxes raised on cooked food diets had significantly less facial growth than animals raised on harder foods. As noted above, the growth difference matrix revealed no interlandmark distances in which the soft food group experienced more growth than the hard diet group. Instead, the hard food animals grew more, particularly in transverse dimensions between the lower face and the zygomatic arch, and between the zygomatic arch and the posterior portions of the cranium. These effects are reflected in the shape differences detected between the two groups. Animals raised on hard food had transversely wider and longer faces primarily along the ventral aspect of the cranium, with correspondingly smaller dimensions of the dorsal portion of the rostrum and between the anterior rostrum and the posterior portions of the face. In addition, the mandibular corpus in the

hard food group was significantly thicker and taller than in the soft food group.

If we consider the strain results along the with data on facial growth rates, then it appears possible that, as predicted, variations in the amounts of regional growth correlate to some extent with regional strain magnitudes. For the most part, dimensions in the more ventral part of the face with the highest strains (particularly the zygomatic), experienced the most growth, and are relatively larger in the hard versus soft diet group. Moreover, as predicted, the major vectors of growth correspond approximately to the observed planes of deformation. As noted above the cranium in the hyrax appears to be predominantly twisted around an anteroposterior axis. The most effective way to counteract twisting is to add mass in the coronal plane at the margins of the face away from the midline axis. While growth in the hyrax skull is evidently complex, the above results (Tables 8 and 9; Figs. 5 and 6) indicate that the hyraxes fed hard food had relatively more growth in posteromedial and anterolateral directions in the more posterior portions of the face. In addition, the mandibular corpus is both dorsoventrally taller and mediolaterally thicker in the hard food group, which would counteract sagittal and lateral transverse bending, respectively. However, no significant differences were evident in the symphysis where lateral transverse bending forces were concentrated (but where no significant difference in hard versus soft foods were measured), highlighting the lack of any simple correspondence between strain magnitudes and growth.

More detailed experiments on larger sample sizes are necessary to confirm the above results. Nonetheless, these data lend support to the hypothesis that masticating softer, more processed (cooked) foods while the animals are growing can lead to reduced facial growth in mammals with retracted molar rows. These data augment the results of previous studies, both experimental (Bouvier and Hylander, 1981; Corruccini and Beecher, 1982, 1984; Yamada and Kimmel, 1991; Ciochon et al., 1997) and comparative (Carlson, 1976; Carlson and Van Gerven, 1977; Ingervall and Helkimo, 1978; Corruccini, 1990; Varrela, 1992) that indicate that a soft food diet stimulates less growth in the cranium, particularly in the mandibular and maxillary arches. However, in contrast to previous experimental studies cited above, this study compared cooked versus dried foods rather than hard versus nearly liquid diets. The results are therefore more comparable in some respects to the biomechanical effects of technological changes in food processing that occurred during the last few thousand years.

One difficult problem that requires further resolution is the extent to which the differences between hyraxes and non-human anthropoids are relevant to human facial biomechanics. We do not wish in any way to suggest that the hyrax is a straightforward analog for human facial biomechanics and growth. As noted above, hyraxes differ from humans and other primates in a number of important features, most crucially in the size and position of much of the face, which in humans is taller, wider, and oriented in the coronal plane. Biomechanically, the greatest difference between hyraxes very prognathic mammals such as swine and most non-human anthropoids that have been studied appears to be the prevalence of twisting in the upper face. The extent to which twisting is a function of postcanine retrognathy or other factors needs to be examined using additional animal models, and will benefit from testing with finite element modeling (e.g., Korioth and Versluis, 1997). However, it is interesting that the size and shape differences documented in this study between hyraxes fed hard and cooked food are both qualitatively and quantitatively comparable to the differences (summarized above) in facial size that have been measured in several human studies (e.g., Corruccini et al., 1985; Ingervall and Bitsanis, 1987; Varrela, 1992; Lieberman, 1998). In particular, after only three months, the mean difference in growth among interlandmark distances in which there were significant contrasts between treatment groups is approximately 9%. These differences mostly were in mandibular corpus size, the size of the maxillary arch, and the position of the zygomatic arch relative to the rest of the face.

In short, these results support the hypothesis that human faces have become relatively smaller despite increases in body size as a result of changes

in mechanical properties of food. Additional research is needed to refine this hypothesis. In particular, larger sample sizes and longer treatment periods should reveal additional and potentially significant results in both the cranium and mandible, and provide more data on the nature and pattern of strains generated by mastication in different regions of the skull and mandible. In addition, further research is needed to determine the relationship between specific parameters of mechanical loading that cooking affects (most notably strain magnitude, number of strain cycles) and rates of site specific growth in the face at sutures and growth fields that generate the differences in facial size and shape documented here and in other studies.

Acknowledgements

We thank Phil Amsterdam, A. Biewener, AW Crompton, Leanne DeNenno, John Landon, Naresh Nayaranaj, Masrour Makaremi, John Polk, Pedro Ramirez, Campbell Rolian, and Lee Tuanquin for their assistance in various aspects of this project. Callum Ross and four anonymous referees provided helpful comments. Financial support was provided by NIH SBIR DE13875-01, the Bioqual Corporation, Harvard University, and the George Washington University.

References

Agrawal, K.R., Lucas, P.W., Prinz, J.F., Bruce, I.C., 1997. Mechanical properties of foods responsible for resisting food breakdown in the human mouth. Arch. Oral Biol. 42, 1–9.

Beecher, R.M., Corruccini, R.S., Freeman, M., 1983. Craniofacial correlates of dietary consistency in a nonhuman primate. J. Craniofac. Gen. Dev. Biol. 3, 193–202.

Bertram, J., Swartz, S.M., 1991. The 'Law of Bone Transformation': A case of crying Wolff? Biol. Rev. 66, 245–273.

Biewener, A.A., 1992. In vivo measurement of bone strain and tendon force. In: Biewener, A.A. (Ed.), Biomechanics—Structures and Systems: A Practical Approach. Oxford University Press, Oxford, pp. 123–147.

Biewener, A.A., Swartz, S.M., Bertram, J., 1986. Bone modeling during growth: Dynamic strain equilibrium in the chick tibiotarsus. Calc. Tiss. Int. 39, 390–395.

Bouvier, M., Hylander, W., 1981. Effect of bone strain on cortical bone structure in macaques (*M. mulatta*). J. Morphol. 167, 1–12.

Bouvier, M., Hylander, W., 1996. The function of secondary osteonal bone. Mechanical or metabolic? Arch. Oral Biol. 41, 941–950.

Brace, C.L., Rosenberg, K., Hunt, K.D., 1987. Gradual change in human tooth size in the late Pleistocene and post-Pleistocene. Evolution 41, 705–720.

Brace, C.L., Smith, S.L., Hunt, K.D., 1991. What big teeth you had grandma! Human tooth size, past and present. In: Kelley, M.A., Larsen, C.S. (Eds.), Advances in Dental Anthropology. Wiley-Liss, New York, pp. 33–57.

Carlson, D.S., 1976. Temporal variation in prehistoric Nubian crania. Am. J. Phys. Anthrop. 45, 467–484.

Carlson, D.S., Van Gerven, D.P., 1977. Masticatory function and Post-Pleistocene evolution in Nubia. Am. J. Phys. Anthrop. 46, 495–506.

Carlsson, G.E., Persson, G., 1967. Morphological changes in the mandible after extraction and wearing of dentures: A longitudinal, clinical and x-ray cephalometric study covering 5 years. Odontol. Rev. 18, 27–54.

Carter, D.R., Beaupré, G.S., 2001. Skeletal Form and Function: Mechanobiology of Skeletal Development, Aging and Regeneration. Cambridge University Press, Cambridge.

Ciochon, R.L., Nisbett, R.A., Corruccini, R.S., 1997. Dietary consistency and craniofacial development related to masticatory function in minipigs. J. Craniofac. Genet. Dev. Biol. 17, 96–102.

Corruccini, R.S., 1984. An epidemiologic transition in dental occlusion in world populations. Am. J. Orthod. 86, 419–426.

Corruccini, R.S., 1990. Australian aboriginal tooth succession, interproximal attrition, and Begg's theory. Am. J. Orthod. Dentofac. Orthop. 97, 349–357.

Corruccini, R.S., Beecher, R., 1982. Occlusal variation related to soft diet in a nonhuman primate. Science 218, 74–76.

Corruccini, R.S., Beecher, R., 1984. Occlusofacial morphological integration lowered in baboons raised on soft diet. J. Craniofac. Genet. Dev. Biol. 4, 135–142.

Corruccini, R.S., Henderson, A.M., Kaul, S.S., 1985. Bite force variation related to occlusal variation in rural and urban Punjabi. Arch. Oral Biol. 30, 65–69.

Crompton, A.W., 1995. Masticatory function in non-mammalian cynodonts and early mammals. In: Thomason, J.J. (Ed.), Functional Morphology in Vertebrate Paleontology. Cambridge University Press, Cambridge, pp. 55–75.

Currey, J.D., 2002. Bones: Structure and Mechanics. Princeton University Press, Princeton.

Daegling, D.J., Hylander, W.L., 1998. Biomechanics of torsion in the human mandible. Am. J. Phys. Anthrop. 105, 73–87.

Dechow, P., Carlson, D., 1983. Occlusal force and craniofacial biomechanics during growth. Am. J. Phys. Anthrop. 83, 219–237.

Demes, B., 1982. The resistance of primate skulls against mechanical stresses. J. Hum. Evol. 11, 687–691.

Demes, B., Creel, N., 1988. Bite force, diet and cranial morphology of fossil hominids. J. Hum. Evol. 17, 657–670.

English, J.D., Buschang, P.H., Throckmorton, G.S., 2002. Does malocclusion affect masticatory performance? Angle Orthod. 72, 21–27.

Engström, C., Kiliaridis, S., Thilander, B., 1986. The relationship between masticatory muscle function and cranial morphology. II.A histological study in the growing rat fed a soft diet. Eur. J. Orthod. 8, 271–279.

Franks, H.A., German, R.Z., Crompton, A.W., Hiiemae, K.M., 1985. Mechanism of intra-oral transport in a herbivore, the hyrax (*Procavia syriacus*). Arch. Oral Biol. 30, 539–544.

German, R.Z., Franks, H.A., 1991. Timing in the movement of jaws, tongue, and hyoid during feeding in the hyrax, *Procavia syriacus*. J. Exp. Zool. 257, 34–42.

Greaves, W.S., 1978. The jaw lever system in ungulates: a new model. J. Zool. Lond. 184, 271–285.

Greaves, W.S., 1985. The mammalian postorbital bar as a torsion-resisting helical strut. J. Zool. Lond. 207, 125–136.

Griner, L.A., 1968. The rock hyrax (*Procavia capensis*): a potential laboratory animal. Lab. Anim. Care 18, 144–150.

Herring, S.W., Rafferty, K.L., Liu, Z.J., Marshall, C.D., 2001. Jaw muscles and the skull in mammals: the biomechanics of mastication. Comp. Biochem. Physiol. A Mol. Integr. Physiol. 131, 207–219.

Herring, S.W., Mucci, R.J., 1991. *In vivo* strain in cranial sutures: the zygomatic arch. J. Morphol. 207, 225–239.

Herring, S.W., Teng, S., 2000. Strain in the braincase and its sutures during function. Am. J. Phys. Anthrop. 112, 575–593.

Herring, S.W., Teng, S., Huang, X., Mucci, R.J., Freeman, J., 1996. Patterns of bone strain in the zygomatic arch. Anat. Rec. 246, 446–457.

Hylander, W.L., 1979. The functional significance of primate mandibular form. J. Morphol. 160, 223–239.

Hylander, W.L., 1984. Stress and strain in the mandibular symphysis of primates: A test of competing hypotheses. Am. J. Phys. Anthrop. 64, 1–46.

Hylander, W.L., 1985. Mandibular function and biomechanical stress and scaling. Am. Zool. 25, 315–330.

Hylander, W.L., 1986. In vivo bone strain as an indicator of masticatory force in Macaca fascilularis. Arch. Oral Biol. 31, 149–157.

Hylander, W.L., 1988. Implications of in vivo experiments for interpreting the functional significance of "robust" australopithecine jaws. In: Grine, F. (Ed.), Evolutionary History of the "Robust" Australopithecines. Aldine De Gruyter, New York, pp. 55–83.

Hylander, W.L., Johnson, K.R., 1992. Strain gradients in the craniofacial region of primates. In: Davidovitch, Z. (Ed.), The Biological Mechanisms of Tooth Movement and Craniofacial Adaptation. Ohio State University College of Dentistry, Columbus, pp. 559–569.

Hylander, W.L., Ravosa, M.J., 1992. An analysis of the supraorbital region of primates: a morphometric and experimental approach. In: Smith, P., Tchernov, E. (Eds.), Structure, Function, and Evolution of Teeth. Freund, Tel Aviv, pp. 233–255.

Hylander, W.L., Johnson, K.R., Crompton, A.W., 1987. Loading patterns and jaw movement during mastication in Macaca fascicularis: A bone strain, electromyographic and cineradiographic analysis. Am. J. Phys. Anthrop. 72, 287–314.

Hylander, W.L., Picq, P.G., Johnson, K.R., 1991a. Masticatory-stress hypotheses and the supraorbital region of primates. Am. J. Phys. Anthrop. 86, 1–36.

Hylander, W.L., Picq, P.G., Johnson, K.R., 1991b. Function of the supraorbital region of primates. Arch. Oral Biol. 36, 273–281.

Hylander, W.L., Ravosa, M.J., Ross, C.F., Wall, C.E., Johnson, K.R., 2000. Symphyseal fusion and jaw-adductor muscle force. Am. J. Phys. Anthrop. 107, 257–271.

Ingervall, B., Bitsanis, E., 1987. A pilot study on the effect of masticatory muscle training on facial growth in long-face children. Eur. J. Orthodont. 9, 15–23.

Ingervall, B., Helkimo, E., 1978. Masticatory muscle force and facial morphology in man. Arch. Oral Biol. 23, 203–206.

Israel, H., 1973. Age factor and the pattern of change in craniofacial structures. Am. J. Phys. Anthrop. 39, 111–128.

Janis, C.M., 1979. Mastication in the hyrax and its relevance to ungulate dental evolution. Paleobiology 5, 50–59.

Janis, C.M., 1983. Muscle of the masticatory apparatus in two genera of Hyrax (*Procavia* and *Heterohyrax*). J. Morphol. 176, 61–87.

Kiliaridis, S., 1989. Muscle function as a determinant of mandibular growth in normal and hypocalcaemic rat. Eur. J. Orthod. 11, 298–308.

Kiliaridis, S., 1995. Masticatory muscle influence on craniofacial growth. Acta Odontol. Scand. 53, 196–202.

Kiliaridis, S., Engström, C., Chavez, L.M.E., 1992. Influence of masticatory muscle function on craniofacial growth in hypocalcemic rats. Scand. J. Dent. Res. 100, 330–336.

Kiliaridis, S., Engström, C., Thilander, B., 1986. The relationship between masticatory muscle function and cranial morphology. I. A cephalometric longitudinal analysis in the growing rat fed a soft diet. Eur. J. Orthodont. 7, 273–283.

Kiliaridis, S., Mejersjö, C., Thilander, B., 1989. Muscle function and craniofacial morphology: a clinical study in patients with myotonic dystrophy. Eur. J. Orthodont. 11, 131–138.

Korioth, T.W.P., Versluis, A., 1997. Modeling the mechanical behavior of the jaws and their related structures by finite element (FE) analysis. Crit. Rev. Oral Biol. Med. 8, 90–104.

Lele, S., 1993. Euclidean Distance Matrix Analysis (EDMA): Estimation of mean form and mean form difference. Mathematical Geology 25, 573–602.

Lele, S., Richtsmeier, J.T., 1991. Euclidean Distance Matrix Analysis: A coordinate-free approach for comparing biological shapes using landmark data. Am. J. Phys. Anthrop. 86, 415–427.

Lele, S., Richtsmeier, J.T., 1995. Euclidean distance matrix analysis: Confidence intervals for form and growth differences. Am. J. Phys. Anthrop. 98, 73–86.

Lieberman, D.E., 1993. Life history variables preserved in dental cementum microstructure. Science 261, 1162–1164.

Lieberman, D.E., 1998. Sphenoid shortening and the evolution of modern human cranial shape. Nature 393, 158–162.

Lieberman, D.E., Crompton, A.W., 2000. Why fuse the mandibular symphysis: A comparative analysis. Am. J. Phys. Anthrop. 112, 517–540.

Lieberman, D.E., Pearson, O.M., Polk, J.D., Demes, B., Crompton, A.W., 2003. Optimization of bone growth and remodeling in response to loading in tapered mammalian limbs. J. Exp. Biol. 206, 3125–3138.

Lucas, P.W., Luke, D.A., 1984. Chewing it over—basic principles of food breakdown. In: Chivers, D.J., Wood, B.A., Bilsborough, A. (Eds.), Food Acquisition and Processing in Primates. Plenum, New York, pp. 283–302.

Lukacs, J.R., 1989. Dental Paleopathology: methods for reconstructing dietary patterns. In: Iscan, M.R., Kennedy, K.A.R. (Eds.), Reconstruction of Life from the Skeleton. Alan R Liss, New York, pp. 261–286.

Martin, R.B., Burr, D.B., Sharkey, N., 1998. Skeletal Tissue Mechanics. Springer, New York.

Moore, W.J., 1965. Masticatory function and skull growth. J. Zool. Lond. 146, 123–131.

Preuschoft, H., Demes, B., Meyer, M., Bar, H.F., 1986. The biomechanical principles realized in the upper jaw of long-snouted primates. In: Else, J.G., Lee, P.C. (Eds.), Primate Evolution. Cambridge University Press, Cambridge, pp. 249–264.

Rafferty, K.L., Herring, S.W., 1999. Craniofacial sutures: morphology, growth, and in vivo masticatory strains. J. Morphol. 242, 167–179.

Rafferty, K.L., Herring, S.W., Marshall, C.D., 2003. Biomechanics of the rostrum and the role of facial sutures. J. Morphol. 257, 233–244.

Rangel, R.D., Oyen, O.J., Russell, M.D., 1985. Changes in masticatory biomechanics and stress magnitude that affect growth and development of the facial skeleton. Prog. Clin. Biol. Res. 187, 281–293.

Ravosa, M.J., Noble, V.E., Hylander, W.L., Johnson, K.R., Kowalski, E.M., 2000a. Masticatory stress, orbital orientation and the evolution of the primate postorbital bar. J hum. Evol. 38, 667–693.

Ravosa, M.J., Johnson, K.R., Hylander, W.L., 2000b. Strain in the galago facial skull. J. Morphol. 245, 51–66.

Richards, M.P., Pettitt, P.B., Stiner, M.C., Trinkaus, E., 2001. Stable isotope evidence for increasing dietary breadth in the European mid-Upper Paleolithic. Proc. Natl. Acad. Sci. 98, 6528–6532.

Richtsmeier, J.T., Lele, S., 1993. A coordinate-free approach to the analysis of growth patterns: Models and theoretical considerations. Biol. Rev. 68, 381–411.

Ross, C.F., 2001. In vivo function of the craniofacial haft: the interorbital "pillar". Am. J. Phys. Anthrop. 116, 108–139.

Ross, C.F., Hylander, W.L., 1996. In vivo and in vitro bone strain in the owl monkey circumorbital region and the function of the postorbital septum. Am. J. Phys. Anthrop. 101, 183–215.

Rubin, C.T., Lanyon, L.E., 1984. Dynamic Strain Similarity in vertebrates: an alternative to allometric limb bone scaling. J. Theoret. Biol. 107, 321–327.

Rübsamen, K., Hume, I.D., Englehard, W.V., 1982. Physiology of the rock hyrax. Comp. Biochem. Physiol. 72A, 271–277.

Shiau, Y.Y., Peng, C.C., Hsu, C.W., 1999. Evaluation of biting performance with standardized test-foods. J. Oral Rehabil. 26, 447–452.

Spencer, M.A., 1999. Constraints on masticatory system evolution in anthropoid primates. Am. J. Phys. Anthrop. 108, 450–483.

Spencer, M.A., 1998. Force production in the primate masticatory system: electromyographic tests of biomechanical hypotheses. J. Hum. Evol. 34, 25–54.

Stiner, M.C., 2001. Thirty years on the "broad spectrum revolution" and paleolithic demography. Proc. Natl. Acad. Sci. 98, 6993–6996.

Stiner, M.C., Munro, N.D., Surovell, T.A., Tchernov, E., Bar-Yosef, O., 1999. Paleolithic population growth pulses evidenced by small animal exploitation. Science 283, 190–194.

Strait, S., 1997. Tooth use and the physical properties of food. Evol. Anthrop. 5, 199–211.

Sugimura, T., Inada, J., Sawa, S., Kakudo, Y., 1984. Dynamic responses of the skull caused by loss of occlusal force. J. Osaka Dental Univ. 18, 29–42.

Varrela, J., 1992. Dimensional variation of craniofacial structures in relation to changing masticatory-functional demands. Eur. J. Orthodont. 14, 31–36.

Wen, P.T., 1984. Electromyographic and Cineradiographic Study of Translation in the Hyrax. Unpub. Thesis: Harvard University.

Wrangham, R.W., Conklin-Brittain, N., 2003. Cooking as a biological trait. Comp. Biochem. Physiol. A 136, 35–46.

Wrangham, R.W., Jones, J.H., Laden, G., Pilbeam, D., Conklin-Brittain, N., 1999. The raw and the stolen. Cooking and the ecology of human origins. Curr. Anthrop. 40, 567–594.

Yamada, K., Kimmel, D.B., 1991. The effect of dietary consistency on bone mass and turnover in the growing rat mandible. Arch. Oral Biol. 36, 129–138.